Electronic Supplementary Information for

Metal ion mediated transition from random coil to β-sheet and aggregation of Bri2-23, the natural inhibitor of Aβ aggregation.

Marek Luczkowski,[†*] Riccardo De Ricco,[‡] Monika Stachura,[§] Slawomir Potocki,[†] Lars Hemmingsen,[§] Daniela Valensin[‡*]

[†]*Faculty of Chemistry, University of Wroclaw, F. Joliot Curie 14, 50-383 Wroclaw, Poland*

[‡]*Department of Biotechnology, Chemistry and Pharmacy, University of Siena, Via A. Moro 2, 53100 Siena, Italy*

[§]*Department of Chemistry, University of Copenhagen, Universitetsparken 5, 2100 Copenhagen, Denmark*

* e-mail: marek.luczkowski@chem.uni.wroc.pl, daniela.valensin@unisi.it

Mass spectrometry analysis of ternary system

We performed mass spectrometry studies of the system in alkaline pH in the presence cysteine as a competing ligand. Our aim was to corroborate the formation of negatively charged ternary complex species in solution. Crude analysis of the data reveal the presence of binary Hg(II) complexes of BRI (m/Z = 941.75 for Z = -3 and 1413.12 for Z = -2) coexisting with various adducts (e.g m/Z = 1482.57 or 1511.55) of its ternary complexes with cysteine (Figure 1S). The detailed isotopic profile of one of these adducts of ternary complex of mercury(II), BRI2-23 and cysteine coalesces with Na^+, Cl^- and NH_4^+ (m/Z = 1511.55) is shown in figure 2S. What is worth to mention, no BRI2-23 complexes of general HgL_2 stoichiometry were detected at this experimental condition. The detection of ternary species corroborates the potentiometrically assessed model and strengthens the consistency of calculated formation constants. Besides, the predominance of ternary complexes in strongly alkaline pH range for corresponding system has been previously reported.[1]

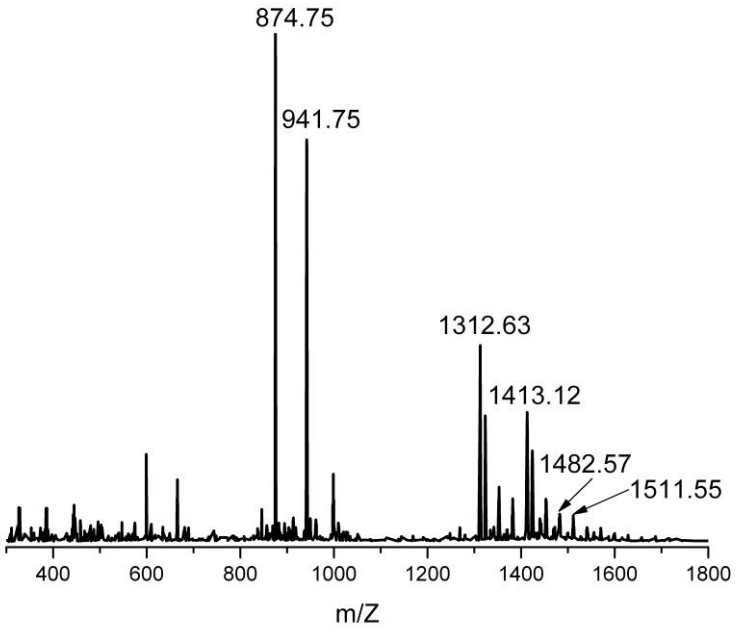

Figure 1S. ESI-MS spectra of Hg(II) complex of BRI2-23 peptide at pH 11 in ammonium hydroxide (0.4M). $c_{BRI2-23}$ = 1 x10^{-4}M; Hg(II)/BRI2-23/Cys ratio 1:1:1; MeOH/H_2O = 1:2.

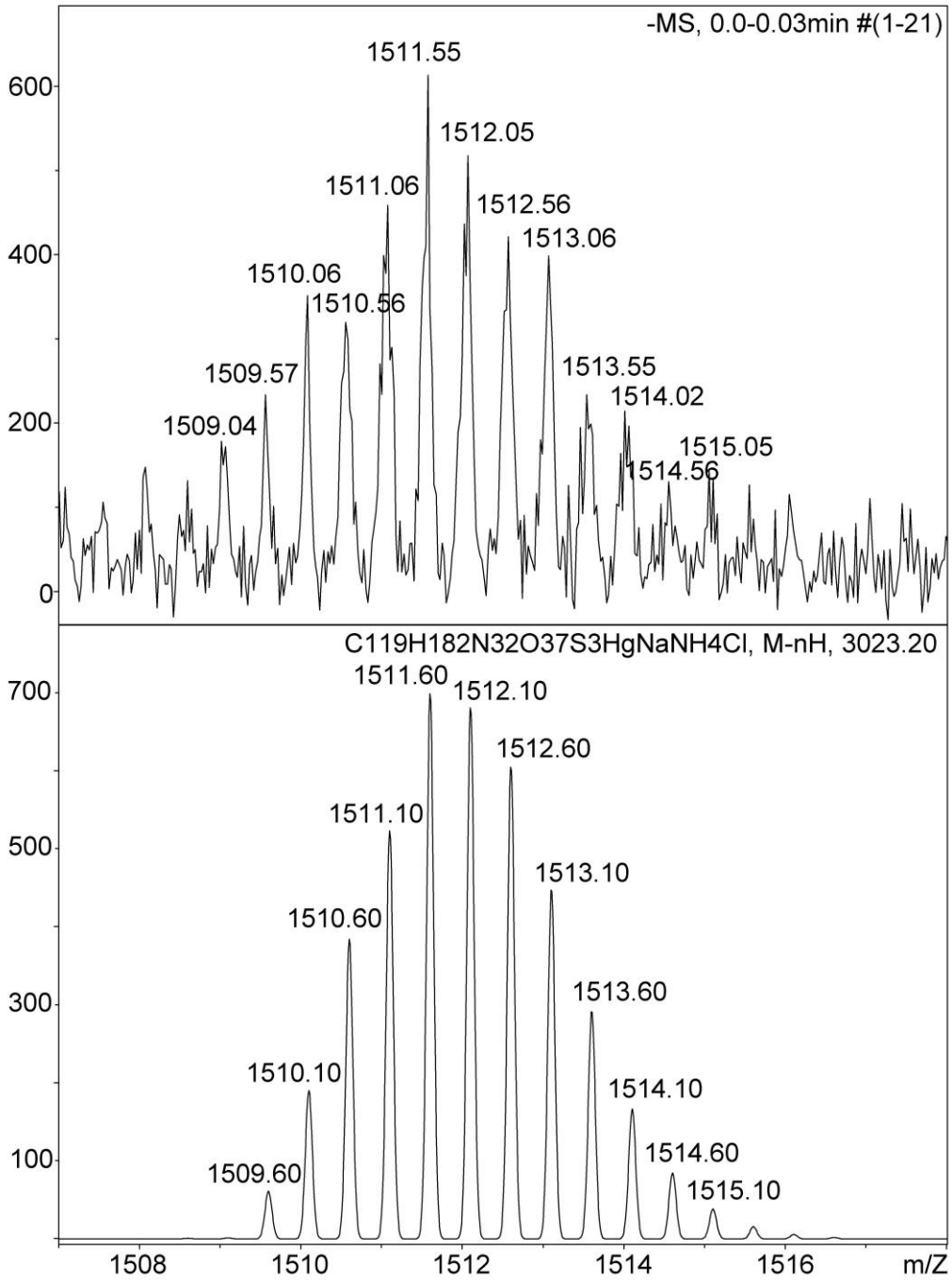

Figure 2S. Isotopic profile of ternary Hg(II) complex species of BRI2-23 and cysteine at pH 11 in ammonium hydroxide (0.4M). [BRI2-23] 1 x10^{-4}M; Hg(II)/BRI2-23/Cys ratio 1:1:1; MeOH/H_2O = 1:2.

Isothermal titration calorimetry

The binding affinity K_a for the Hg(II) complexes of BRI2-23, and their associated thermodynamic parameters are summarized in Figure 3S.

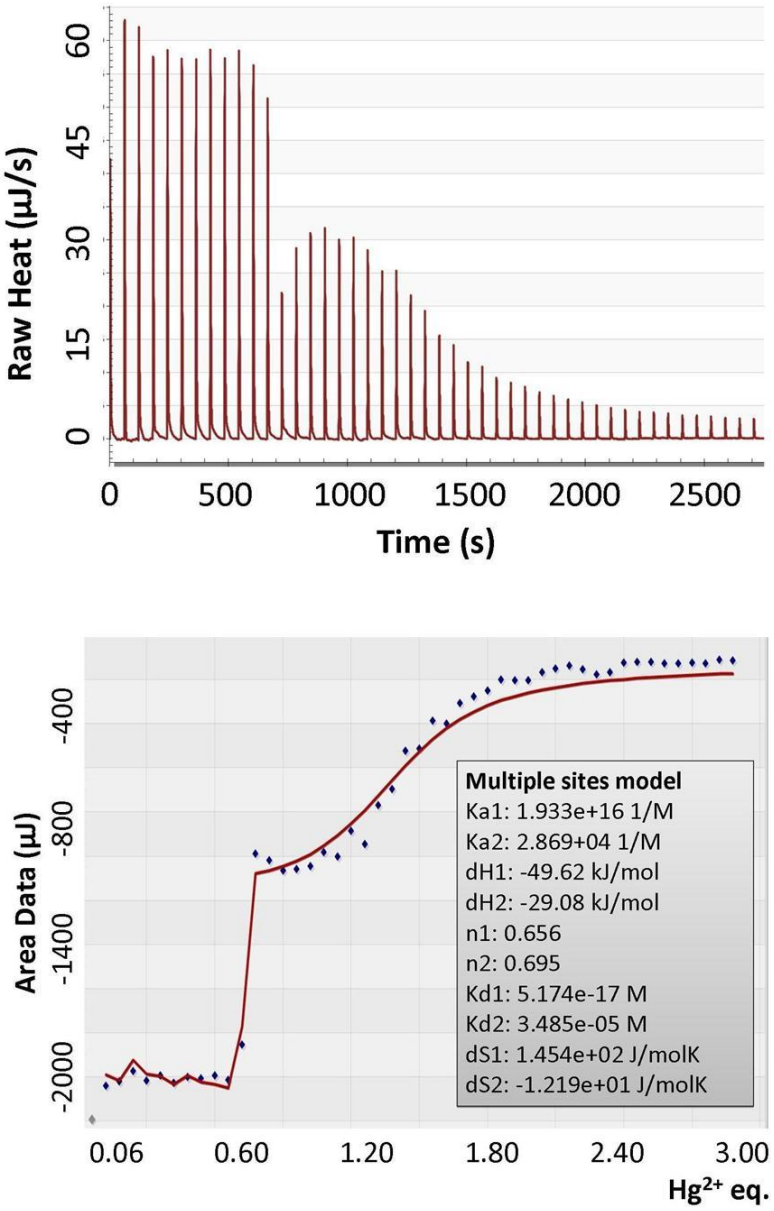

Figure 3S. Total measured heat associated with titration of BRI peptide with Hg(II) (upper panel), and the binding isotherm derived from the enthalpy of each injection in the function of molar Hg(II) equivalents (lower panel).

BRI2-23 peptide shows two exothermic phenomena while titrated with Hg(II), analogically to previously reported other cysteinyl peptides.[2-4] A strong exothermic association is identified at the beginning of each titration of Hg(II) into BRI2-23 peptide. This may reflect the formation of Hg–S coordinate bond(s) that yield exceptionally high K_a formation constants. This would be consistent with the binding preferences of mercury(II), a soft acid that has a tendency to form linear thiolate complexes.[5-6] K_a for Hg(II) and thiols interaction is usually a number to the power of over a dozen,[4] what is not an optimal range for Nano-ITC instrument. The c parameter (defined in this case as $[BRI]/K_d$] equals to 9.66 x 10^{12}, what is much too high for the optimal value.[7] Moreover, as shown in Figure 3S, the curve fitting for this very tight first binding is limited to 1-2 data points. For these two reasons, the association constant for this particular interaction is adapted from the potentiometric data and kept constant during the calculations of other thermodynamic parameters.[8] As we know from MS and NMR spectra evaluation, intramolecular complexes are exclusively formed at low (~ 0.5) metal content. Superficial analysis of ITC plot, that clearly shows two processes, indicates that formation of equimolar species is indistinguishable from formation of further intermolecular complex species, while formation of metal induced organized structures are observed above 0.7 Hg^{2+}/BRI molar ratio. This is with good agreement with NMR data (*vide infra*) that signify the mixture of metallic species at 0.7 Hg^{2+}/BRI molar ratio followed by formation of highly organized structures. We assume that some other indistinguishable inter-molecular phenomenon occurs. The second K_a binding constant ($2.9e^4$/M) reflects the binding of subsequent Hg(II) ions followed by structural rearrangement of the peptide backbone. However, since the exact complex species composition and their distribution profile at higher Hg(II) concentration is not known, the impact of metal sequestration and structural rearrangement of the peptide cannot be readily distinguished in energy profile. We believe that many factors contribute to the thermodynamic

profile of BRI2-23 interaction with Hg(II) ions. On the top of previously mentioned, seed formation leading to aggregation is highly possible scenario. Finally, from the thermodynamic point of view system is saturated when Hg(II)/BRI molar ratio reaches 2.

The large heat flow induced during the first step of the interaction of Hg^{2+} ions with BRI peptide results in exceedingly high enthalpy change ΔH_1 = -49.62 kJ/mol, what suggests strongly that thiol of cysteine residues are the binding sites. Interactions between soft acceptor and soft donor are typically strongly exothermic.[9] The positive entropy, ΔS_1 = 0.145 kJ/mol, may indicate the formation of disordered structure, where main driving forces are hydrophobic interactions and associated release of water. However, large enthalpic contribution shows, that this is an enthalpy-controlled thermodynamic process where the formation of coordinate and hydrogen bonds together with van der Waals interactions play an critical role. The negative value of ΔH and positive value of ΔS indicate highly spontaneous process ($\Delta G^o = \Delta H^o - T\Delta S^o$). The second process is described with the following set of parameters: $K_{d2} = 3.49 \times 10^{-5}$, ΔH_1 = -29.08 kJ/mol and ΔS = -0.012 kJ/mol. As for the lower Hg(II)/BRI2-23 ratios, the enthalpic factor predominates indicating high coordinate and hydrogen bonds impact on the new structure formation, whereas negative entropy reveals different nature of the interaction and the formation of higher, well organized, intermolecular structures.

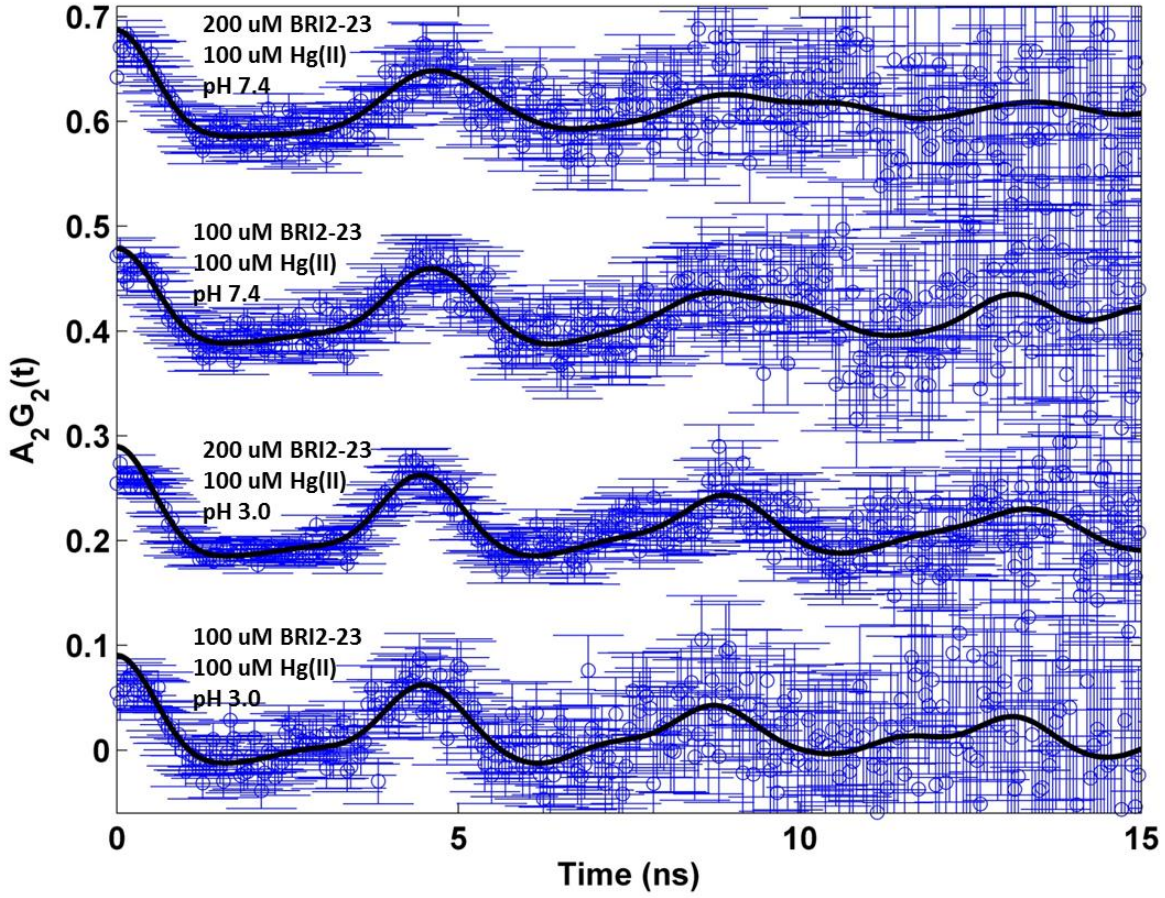

Figure 4S. ^{199m}Hg PAC data for BRI2-23 under the indicated experimental conditions. Blue: Experimental data-points with error bars; black: Fit with the NQI parameters presented in Table 1S.

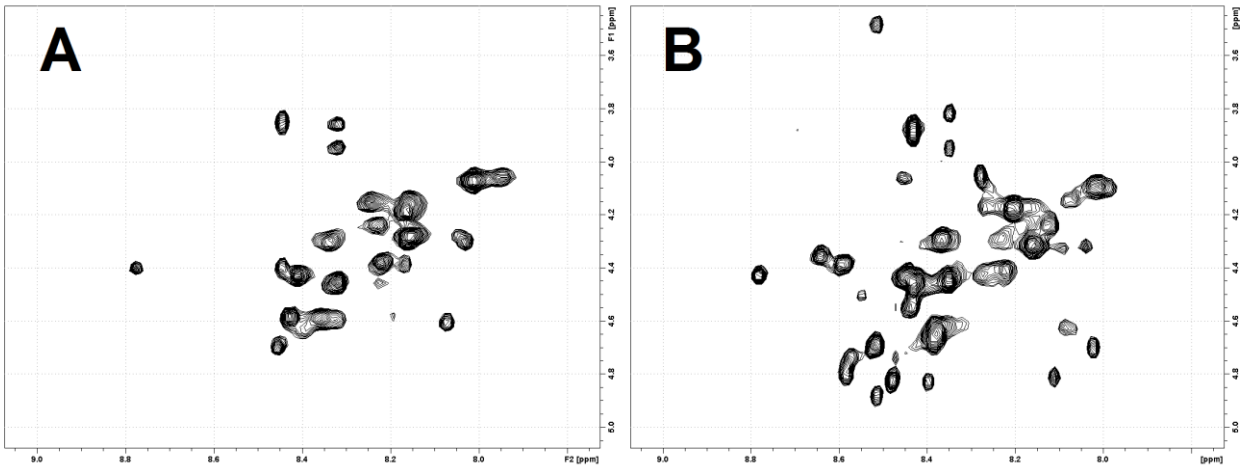

Figure 5S. 2D ^{1}H-^{1}H TOCSY spectra (NH-Hα region) of Bri2-23 0.5mM in H_2O:D_2O 90:10 at 298K and pH 3.0 in presence of A) 0.9 equivalents of Ag(I) ions; B) 0.9 equivalents of Hg(II) ions.

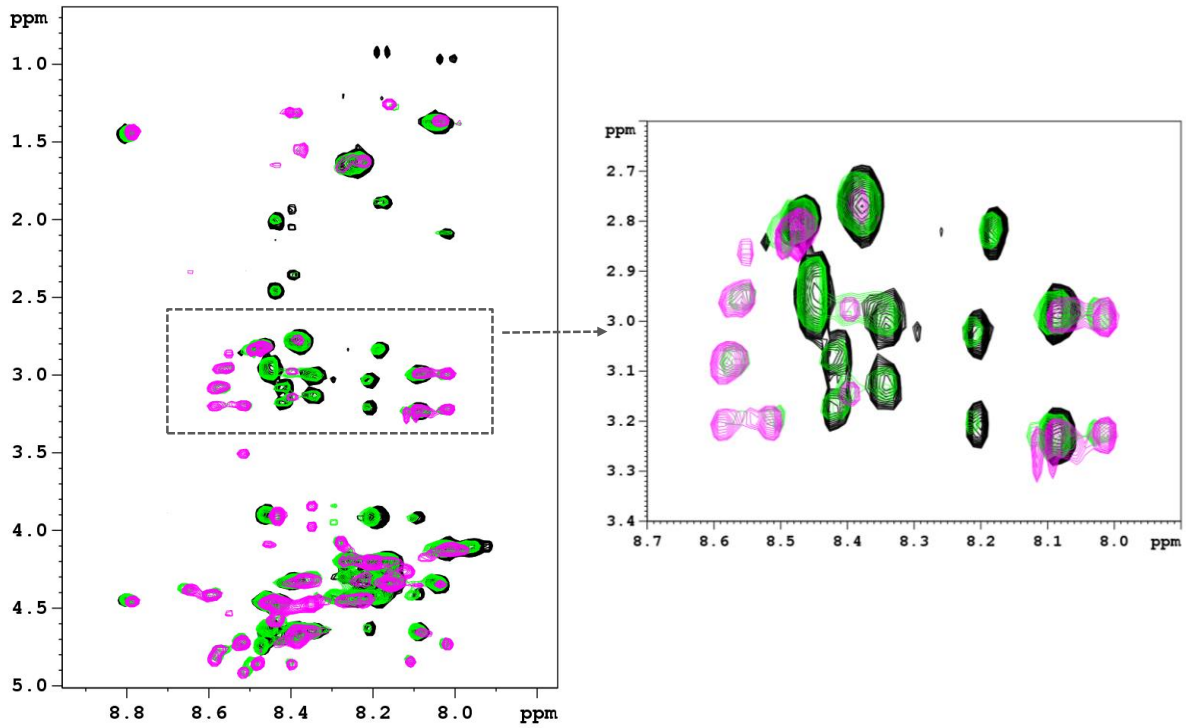

Figure 6S. 2D ^{1}H-^{1}H TOCSY spectra of Bri2-23 0.5mM in H_2O:D_2O 90:10 at 298K and pH 3.0 (black) in presence of 0.5 equivalents of Hg(II) ions (green); in presence of 0.9 equivalents of Hg(II) ions (magenta).

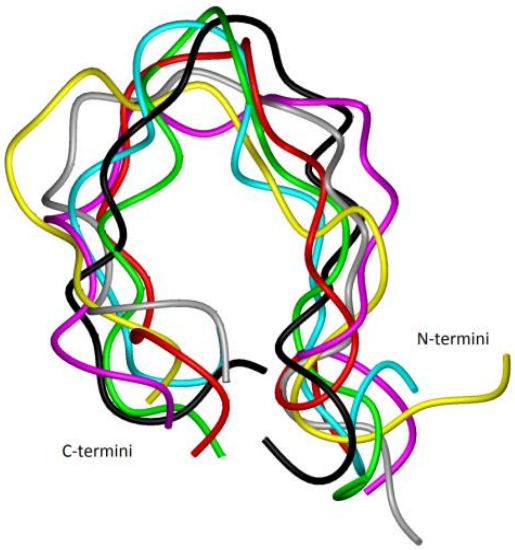

Figure 7S. Superimposed selected structures obtained by NMR DYANA calculation.

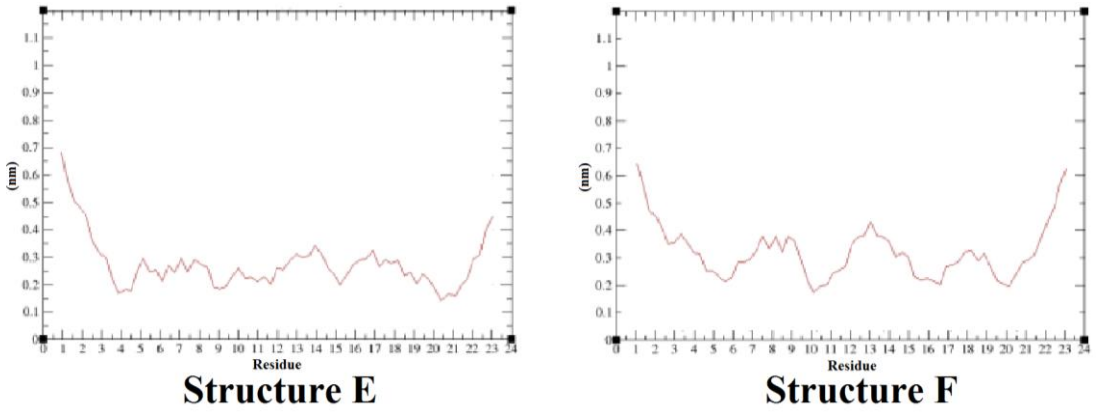

Figure 8S. RMS fluctuation calculated for each residues of structures E and F.

Table 1S. Parameters fitted to PAC-data. The numbers in parenthesis are the standard deviations of the fitted parameters.

BRI	Hg(II)	pH	ν_Q	η	$\Delta\omega_0/\omega_0$	$1/\tau_c$	A	χ_r^2
μM	μM		GHz		×100	us^{-1}	×100	
200	100	7.4	1.47(8) 1.25(6)	0.1(1) 0f	7(5) 0(10)	0(15)	12(6) 2(5)	0.62
100	100	7.4	1.51(6) 1.32(4)	0.18(6) 0.19(7)	2(4) 0(5)	0(17)	8(5) 5(5)	0.59
200	100	3.0	1.48(1)	0.18(2)	3.6(9)	18(9)	15.3(9)	0.79
100	100	3.0	1.51(5) 1.32(14)	0.24(5) 0.2(1)	0(5) 4(9)	20(23)	9(10) 6(10)	0.50

Table 2S. ^{1}H Chemical Shift of Bri2-23 0.5mM in H_2O:D_2O 90:10 at 298K and pH 3.0

Free	NH	Ha	Hb	Hg	Hd	other	other
Glu-1	nd	4,08	2,11	2,53			
Ala-2	8,79	4,42	1,42				
Ser-3	8,46	4,41	3,87				
Asn-4	8,47	4,71	2,78			6,90	7,58
Cys-5	8,19	4,41	2,81				
Phe-6	8,21	4,61	3,09			7,25	7,34
Ala-7	8,07	4,28	1,34				
Ile-8	7,95	4,08	1,81	1,17	0,82		
Arg-9	8,26	4,26	1,66	1,50	1,57	7,14	3,14
His-10	8,42	4,65	3,10			8,56	7,16
Phe-11	8,35	4,62	3,04			7,32	7,22
Glu-12	8,36	4,30	1,97	2,36			
Asn-13	8,37	4,60	2,76			6,96	7,61
Lys-14	8,27	4,16	1,63	1,19	1,58	2,90	7,50
Phe-15	8,09	4,61	3,06			7,26	7,34
Ala-16	8,05	4,31	1,36				
Val-17	8,03	4,09	2,06	0,94			
Glu-18	8,43	4,44	2,04	2,45			
Thr-19	8,18	4,30	4,15	1,18			
Leu-20	8,24	4,39	1,59	1,59	0,88		
Ile-21	8,18	4,20	1,87	1,19	0,89		
Cys-22	8,45	4,60	2,93				
Ser-23	8,31	4,45	3,91				

Table 3S. Chemical Shift of Bri2-23 0.5mM in H_2O:D_2O 90:10 at 298K and pH 3.0 in presence of 0.7 eqs. of HgII ions (X form)

X-form	NH	Ha	Hb	Hg	Hd	other	other
Glu-1	nd	4,09	2,18	2,55			
Ala-2	8,79	4,43	1,43				
Ser-3	8,44	4,47	3,89				
Asn-4	8,49	4,84	2,82			6,91	7,58
Cys-5	8,40	4,70	3,30				
Phe-6	8,12	4,82	3,10			7,17	7,29
Ala-7	8,41	4,68	1,31				
Ile-8	8,37	4,30	1,79	1,17	0,80		
Arg-9	8,45	4,56	1,65	1,40	1,51	7,15	3,11
His-10	8,59	4,79	3,11			8,58	7,29
Phe-11	8,41	4,84	3,01			7,30	7,17
Glu-12	8,65	4,36	1,99	2,33			
Asn-13	8,56	4,51	2,90			6,99	7,64
Lys-14	8,29	4,05	1,69	1,18	1,57	2,90	7,49
Phe-15	8,03	4,70	3,09			7,27	7,36
Ala-16	8,17	4,32	1,26				
Val-17	8,02	4,10	2,08	0,94			
Glu-18	8,43	4,44	2,05	2,45			
Thr-19	8,46	4,45	4,07	1,16			
Leu-20	8,43	4,60	1,58	1,54	0,81		
Ile-21	8,61	4,39	1,79	nr	0,87		
Cys-22	8,52	4,89	3,34				
Ser-23	8,36	4,46	3,89				

Table 4S. Chemical Shift of Bri2-23 0.5mM in H_2O:D_2O 90:10 at 298K and pH 3.0 in presence of 0.7 eqs. of HgII ions (Y form)

Y-form	NH	Ha	Hb	Hg	Hd	other	other
Glu-1							
Ala-2							
Ser-3							
Asn-4	8,40	4,63	2,76			6,93	7,61
Cys-5							
Phe-6							
Ala-7							
Ile-8							
Arg-9	8,23	4,26	1,68	nr	nr	7,15	3,14
His-10							
Phe-11							
Glu-12	8,46	4,31	1,98	2,36			
Asn-13	8,37	4,63	2,81			6,99	7,63
Lys-14	8,27	4,09	1,62	nr	nr	nr	nr
Phe-15	8,08	4,63	3,09		da def	7,27	7,36
Ala-16	8,05	4,32	1,36				
Val-17	8,09	4,20	1,88	0,91			
Glu-18	8,52	4,69	1,96	2,33			
Thr-19	8,28	4,31	4,17	1,19			
Leu-20	8,24	4,41	1,61	nr	0,87		
Ile-21	8,22	4,19	1,95	1,20	0,87		
Cys-22							
Ser-23							

References:

1. S. Pires, J. Habjanic, M. Sezer, C. M. Soares, L. Hemmingsen, O. Iranzo, *Inorg. Chem.*, 2012, **51**, 11339-11348.
2. X. L. Lin, J. Brooks, M. Bronson, M. Ngu-Schwemlein, *Bioorg. Chem.*, 2012, **44**, 8-18.
3. M. Ngu-Schwemlein, W. Gilbert, K. Askew, S. Schwemlein, *Bioorg. Med. Chem.*, 2008, **16**, 5778-5787.
4. M. Ngu-Schwemlein, J. K. Merle, P. Healy, S. Schwemlein, S. Rhodes, *Thermochim. Acta*, 2009, **496**, 129-135.
5. R. Strand, W. Lund, J. Aaseth, *J. Inorg. Biochem.*, 1983, **19**, 301-309.
6. W. Stricks, I. M. Kolthoff, *J. Am. Chem. Soc.*, 1953, **75**, 5673-5681.
7. W. B. Turnbull, A. H. Daranas, *J. Am. Chem. Soc.*, 2003, **125**, 14859-14866.
8. H. Kozlowski, M. Luczkowski, M. Remelli, *Dalton Trans.*, 2010, **39**, 6371-6385.
9. D. J. Yang, S. O. Shi, L. F. Zheng, T. M. Yao, L. N. Ji, *Biopolymers*, 2010, **93**, 1100-1107.